Rheology of defect networks in cholesteric liquid crystals

Laurence Ramos,* Martin Zapotocky,† T. C. Lubensky, and D. A. Weitz‡
Department of Physics and Astronomy, University of Pennsylvania, Philadelphia, Pennsylvania 19104
(Received 3 August 2001; published 25 September 2002)

The rheological properties of cholesteric liquid crystals containing networks of defects are investigated. A network of linear defects of the ''oily-streak'' type is stabilized when colloidal particles are dispersed into the cholesteric liquid crystals. This network converts the rheological response of a presheared cholesteric liquid crystal from fluidlike to solidlike and leads to the formation of a ''defect-mediated'' solid. The frequency-dependent complex shear modulus $G^*(\omega)$ is measured, for samples with and without inclusions, in both the linear and nonlinear viscoelastic regimes. The linear elastic response mediated by the defect network is discussed in terms of a model analogous to the theories of rubber elasticity. All our data for $G^*(\omega)$ are fitted to a simplified theoretical form, and the values and variations of the fitting parameters, in the various regimes investigated, are discussed in terms of the properties of defect structure present in the samples. Similar rheological properties are expected to arise from particle-stabilized oily-streak defect networks in layered systems such as smectic-*A* and lyotropic L_α phases.

DOI: 10.1103/PhysRevE.66.031711 PACS number(s): 61.30.Jf, 82.70.−y, 83.60.Bc, 83.60.−a

I. INTRODUCTION

Defects are an inherent feature of all systems with long-range order and play a crucial role in determining many properties of these materials. In particular, defects are known to have a dramatic effect on the mechanical properties of a material. In this paper, we study the rheological properties of defect structures in cholesteric liquid crystals. As an introduction to the system, we show an optical microscopy photograph (Fig. 1) that illustrates many of its key properties and that can serve as a motivation for the remainder of the paper. Figure 1 shows a thin film of a cholesteric liquid crystal between two glass plates, in the presence of colloidal inclusions of size exceeding the cholesteric pitch *p*. In the absence of inclusions the sample exhibits the defect-free cholesteric ordering; by contrast, the sample with colloidal inclusions exhibits a dense network of linear defects (Fig. 1) with colloidal inclusions located exclusively at the nodes of the network. These defects are of the ''oily-streak'' type, and are stabilized by the presence of the solid colloidal particles. In Fig. 1, the structure is strongly deformed due to the passage (in approximately the horizontal direction) of a large air bubble moving through the sample. Once the bubble disappears from the field of view, however, the network regains its original, undeformed configuration. This indicates that the defect network structure possesses elastic properties.

The goal of this paper is to investigate systematically how the viscoelastic properties of a cholesteric liquid crystal are changed in the presence of colloidal inclusions, and to understand those changes in terms of the properties of oily-streak-type defect networks. The paper is organized as follows. In Sec. II, we provide a general theoretical background and recall the main results reported previously [1] on cholesteric thin films with and without inclusions. In Sec. III, we demonstrate experimentally that at low frequencies and low strain amplitudes, an aligned bulk cholesteric liquid crystal subjected to a shear parallel to the cholesteric layers exhibits a solidlike behavior when a defect network is present with a higher elastic modulus than when no network is present. We present the observed frequency dependence of the complex shear modulus in both the linear and nonlinear viscoelastic regimes, and contrast the robustness of gel-like behavior in cholesteric liquid crystals with colloidal inclusions to that of pure cholesteric liquid crystals in a state with a nonoriented texture. In Sec. IV, we briefly discuss the origins of viscoelasticity of oily-streak defect networks and compare them to those of crosslinked macromolecular networks in rubber-like solids. We argue that in the linear viscoelastic regime, a rubber-type elasticity model is applicable to the cholesteric system with defects. We then compare our measurements, obtained in the linear viscoelastic regime, to this model, combined with the theory of intrinsic viscoelasticity of

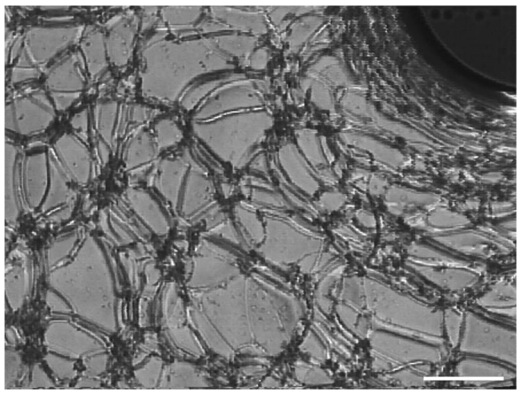

FIG. 1. Air bubble passing through the defect gel network in a system of thickness $H=20$ μm. The bubble travels at an angle of 10° clockwise from the horizontal direction. Scale bar is 100 μm.

*Present address: Groupe de Dynamique des Phases Condensées (UMR CNRS-UM2 5581), CC26, Université Montpellier 2, 34095 Montpellier Cedex 5, France.

†Present address: Center for Studies in Physics and Biology, The Rockefeller University, 1230 York Avenue, New York, NY 10021.

‡Present address: Department of Physics and DEAS, Harvard University, Cambridge, MA 02138.

 ©2002 The American Physical Society

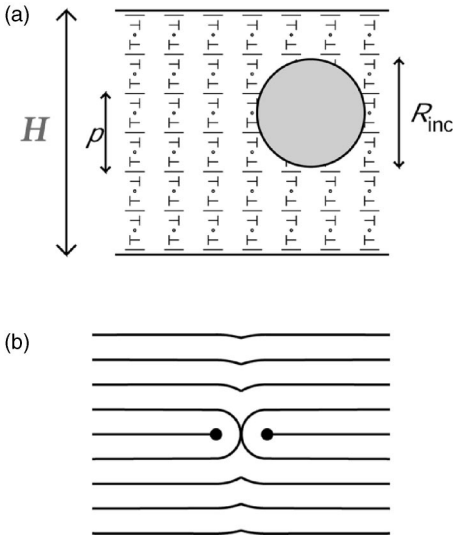

FIG. 2. (a) The planar texture configuration of a cholesteric liquid crystal of pitch p and film thickness H. The cholesteric pitch axis **t** is oriented perpendicular to the film surfaces, and the elongated molecules undergo a helical rotation while staying perpendicular to this axis (the molecules drawn with ''nail heads'' are tilted out of the page by 45°, with the nail head end towards the front of the page). When colloidal inclusions of size $R_{inc} > p$ are added into the system, this ideal planar structure is modified and a planar network of linear defects is stabilized. (b) Arrangement of cholesteric layers in the cross sections of a symmetric oily streak in the planar texture geometry.

defect-free cholesteric liquid crystals. We analyze the data for the frequency-dependent complex shear modulus in both the linear and nonlinear regimes. We employ fitting functions motivated by our model and discuss the values of the fitting parameters in terms of the defect structure of the samples.

II. THE PARTICLE-STABILIZED DEFECT NETWORK

A cholesteric liquid crystal [2] is composed of elongated molecules with chiral interactions. In the cholesteric phase, the molecules have no translational order, but possess long-range orientational order, which can be characterized through the ''director'' field, $\mathbf{n}(\mathbf{r})$, defined as the locally-averaged orientation of the molecules at position $\mathbf{r}$. In contrast to nematic liquid crystals [2], where the director $\mathbf{n}$ is independent of position in the lowest-energy state, in cholesteric liquid crystals $\mathbf{n}(\mathbf{r})$ undergoes a uniform rotation in a particular direction, $\mathbf{t}$, the cholesteric twist axis [see Fig. 2(a)]. The distance p along this axis in which the director undergoes a rotation of 360° is defined as the cholesteric pitch. In the lowest energy state, a cholesteric liquid crystal can therefore be regarded as a structure of equally spaced planes sharing a common molecular orientation, the layer spacing being $p/2$ [Fig. 2(a)].

Departures from this ideal structure lead to a cost in the bulk free energy density which is usually written in terms of the director field $\mathbf{n}(\mathbf{r})$ [2]. We can, however, still define ''cholesteric layers'' in the deformed structure as connected surfaces that are everywhere normal to the local direction of the cholesteric twist axis $\mathbf{t}$. The free energy density can then be viewed as arising from the bending of the layers and from the deviations of their distance from $p/2$. For the purposes of this paper, it will be convenient to describe the configuration of a cholesteric liquid crystal in terms of the ''cholesteric layers,'' rather than directly in terms of the director field $\mathbf{n}(\mathbf{r})$.

We thus view a cholesteric liquid crystal as a layered medium [3] and write its bulk free energy density in the generic form appropriate for lamellar systems (see, e.g., Ref. [4]),

$$f_{\mathrm{lam}} = \frac{1}{2}K\left(\frac{1}{R_1}+\frac{1}{R_2}\right)^2 + \overline{K}\left(\frac{1}{R_1 R_2}\right) + \frac{1}{2}B\epsilon^2, \qquad (1)$$

where R_1 and R_2 are the local values of the principal radii of curvature of the layers, K is the mean bending rigidity, $\overline{K}$ is the Gaussian bending rigidity, B is the compression modulus, and $\epsilon \equiv \delta h/h$ is the local relative variation in layer spacing h. It can be formally shown [5] that for small layer deformations, the cholesteric free energy can be written as Eq. (1) with $K=(3/16)K_{33}$ and $B=(2\pi/p)^2 K_{22}$, where p is the cholesteric pitch and the elastic constants K_{33} and K_{22}, respectively, are the bend and twist elastic constants in the director-based description [2].

In a previous work [1], we demonstrated through direct optical observations that in thin cholesteric films (thickness H of the order of p), a dense planar network of linear defects can be stabilized by the introduction of colloidal inclusions of size R_{inc} exceeding the pitch p of the cholesteric liquid crystal. Moreover, optical observations of thicker samples (H of order $10p$) show a three-dimensional network of linear defects with a structure similar to that of the network in thin samples [6]. The linear defects are ''oily streaks,'' the most common type of defects observed in layered structures in the planar geometry. ''Symmetric'' oily streaks (predominant in thin film samples) can be viewed as being composed of two disclination lines of strength $+1/2$ with an equal number of layers rotating about each disclination line; the structure of such a defect is illustrated in Fig. 2(b). The oily streak has an elastic energy per unit length, or line tension, which is given approximately [1] by the mean bending rigidity K in Eq. (1). We have shown that in bulk samples the stabilized defect network converts a system that is fluidlike in the absence of defects to a *defect-mediated solid* characterized by a gel-like rheology at low frequencies [1]. Our understanding of this behavior is based on viewing a cholesteric liquid crystal as a lamellar medium [3], and similar phenomena are therefore expected to occur in other types of layered materials. Consistent with this, stabilized oily-streak-type defect networks have also been observed in lyotropic L_α phases and found to alter the rheological properties of the system [7,8].

III. EXPERIMENTAL RESULTS

A. Generalities

The cholesteric liquid crystal studied consists of a mixture of cyanobiphenyls doped with chiral molecules. The amount of chiral dopant sets the equilibrium pitch p of the sample, which is measured using the conventional Cano wedge tech-

nique [2]. In our experiments, we use samples with $p = 15\ \mu$m. As colloidal inclusions, we use silica particles of diameter 1 μm. Once incorporated into the liquid crystal, they form clusters of typical size 10–30 μm. We use a Rheometrics strain-controlled rheometer (model Ares), with a 10 g cm transducer in the double-wall Couette geometry, with an inner gap of 1 mm and an outer gap of 1.17 mm. Two types of experiments are performed. Oscillatory measurements are made at a constant strain amplitude γ over a frequency range from 0.01 to 100 rad/sec, and the storage, or elastic modulus, $G'(\omega)$, and the loss modulus, $G''(\omega)$, are determined. In addition, the apparent viscosity η of the samples was determined from the ratio of the measured stress σ to the applied shear rate $\dot{\gamma}$, using steady rate sweep experiments, from 0.015 to 100 $\sec^{-1}$.

B. Nonaligned samples

In the first set of experiments, the samples are submitted to the following thermal treatment: they are first heated up to 70 °C , which is above the isotropic transition temperature ($T_c \simeq 63$ °C) and then quenched to 20 °C. All measurements are performed after the quench at a temperature of 20 °C. We note that the time required for the temperature of the sample to decrease from 70 °C to the transition temperature T_c is less; while the time required to decrease the temperature to 20 °C is much longer (about 20 minutes). This larger cooling time does not, however, appear to affect our results since we do not observe any changes in the data over a period of 10 h following the quench. This is consistent with the measurements of the rate of coarsening of the defects found for thin films [1], where the time needed to obtain a defect-free sample after a temperature quench varies exponentially with the thickness H of the cholesteric sample. We expect that the coarsening time of the defect structure in bulk samples is very long compared to the typical experimental time. This suggests that there should not be any observable changes in the density of defects on the time scale of our experiments. Cholesteric samples with and without inclusions are studied.

We first determine the regime of linear viscoelasticity by making oscillatory measurements in which the maximum strain amplitude, γ, is increased from 10^{-3} to 1, for frequencies of 0.1 rad/sec and 1 rad/sec. As shown in Fig. 3 for $\omega = 1$ rad/sec, up to a maximum strain amplitude of about 0.06, both G' and G'' do not depend on the amplitude of the applied strain, setting the upper limit of the linear regime. The storage and loss moduli are then measured as a function of frequency in the linear regime, using $\gamma = 0.05$, and the experimental results are shown in Fig. 4. There is an exact superposition of the data obtained with pure cholesteric samples and with cholesteric samples containing colloidal inclusions. The materials exhibit a behavior very similar to that of gels. At low frequencies the elastic modulus G' reaches a plateau, G_0, where $G_0 = 1$ dyn/cm^2, and the elastic modulus is larger than the loss modulus G''. At high frequencies a fluidlike behavior is recovered, with a loss modulus G'' larger than the elastic modulus G'. At a critical frequency $\omega_c = 1$ rad/sec, there is a crossover from the solidlike regime where $G' > G''$ and the fluidlike regime where $G'' > G'$.

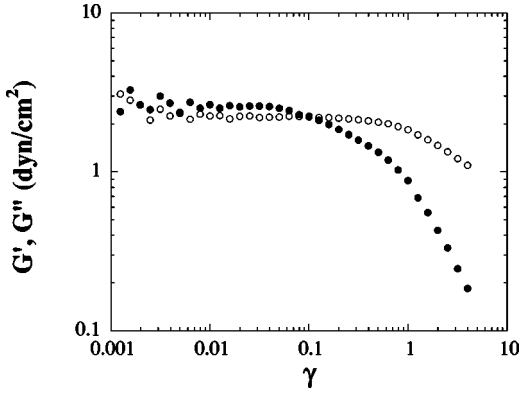

FIG. 3. The strain amplitude dependence of the storage G' (solid circles) and the loss G'' (open circles) moduli for a quenched sample. Measurements were performed at a frequency $\omega = 1$ rad/sec.

The gel-like behavior explains the ability of a bulk cholesteric sample to suspend colloidal particles. Moreover, this rheological behavior agrees qualitatively with previous observations for other layered mesophases, such as small molecules and polymeric smectic phases under equivalent experimental conditions [9,10]. Our moduli are three or four orders of magnitude smaller than those of typical smectics. The rheological response we obtain is consistent with the samples being in a completely randomly oriented state, induced by the thermal quench. In the randomly oriented texture, with an isotropic distribution of the cholesteric layers, the material is sheared in a direction that is not parallel to the layers in most of the sample. This leads to relative changes in the layer spacing of the order of γ and to a compression energy cost of the order $B\gamma^2$ per unit volume, where B is the compression modulus of the layered medium. This corresponds to a stress of the order of $B\gamma$ and consequently to a modulus of the order of B. In cholesteric liquid crystals, the compression modulus is related to the bending modulus K and the cholesteric pitch p by $B = K(2\pi/p)^2$ [5]. Taking the

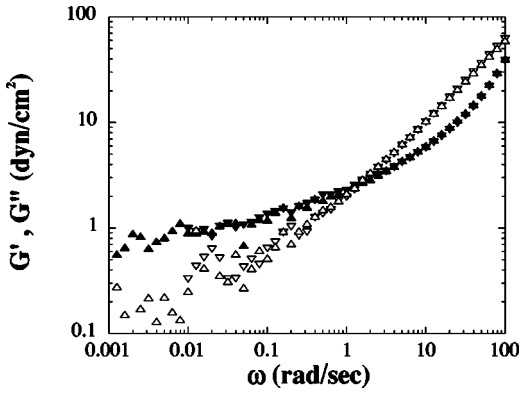

FIG. 4. The frequency dependence of the storage G' (solid symbols) and the loss G'' (open symbols) moduli of a pure cholesteric sample (upwards triangles) and a cholesteric sample with inclusions (downwards triangles). The strain amplitude is $\gamma = 0.05$. Both samples were first submitted to a temperature quench.

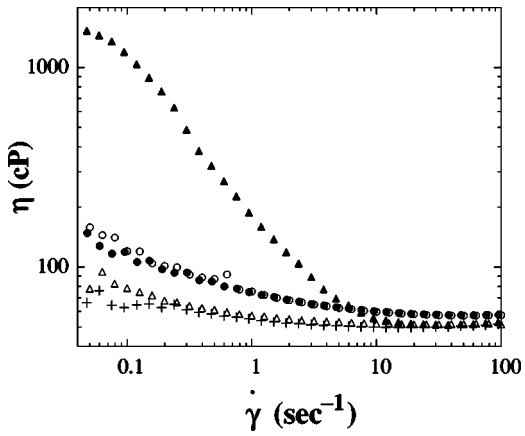

FIG. 5. The shear-rate dependence of the effective viscosity η for a pure cholesteric sample (pluses), and a cholesteric sample with inclusions (circles), which were both presheared (for 500 sec at $\dot{\gamma}=10\ \mathrm{sec}^{-1}$), and for a pure cholesteric sample that was submitted to a temperature quench (triangles). For the quenched sample (triangles), the solid symbols represent the measurements performed right after the quench with the shear rate increasing from low to high values of $\dot{\gamma}$ (increasing), while the open symbols represent the measurements performed decreasing (from high to low $\dot{\gamma}$) subsequent to the increasing scan. The quenched sample exhibits a strong shear thinning along the increasing scan, and a very weak one in the decreasing scan. The decreasing data exactly superimpose with those of the presheared pure cholesteric sample (pluses); consecutive runs give the same results. The presheared sample with inclusions exhibits an intermediate shear-thinning that is reversible: the increasing (solid circles) and decreasing (open circles) sweeps give similar results.

value $K\simeq 10^{-6}$ dyn, typical for cholesteric liquid crystals, we find B to be of the order of 10 dyn/cm^2, in rough agreement with the experimentally measured value of $G_0=1$ dyn/cm^2.

Steady rate sweep experiments are performed after the thermal quench. We first scan from low to high shear rates and then from high to low shear rates. Again, pure cholesteric samples and cholesteric samples with inclusions give exactly the same responses for the increasing shear rates. As shown in Fig. 5, the samples exhibit a strong shear thinning, with the effective viscosity decreasing from 15 P down to 50 cP. A constant value of viscosity is reached in this particular experiment at a shear rate $\dot{\gamma}\simeq 10\ \mathrm{sec}^{-1}$. In sharp contrast, as the shear rate is decreased, the pure cholesteric sample exhibits only a weak variation of its effective viscosity, with changes by about 20%. Moreover, samples containing colloidal inclusions exhibit a different behavior (see following subsection). These experiments indicate that the application of a shear rate induces a strong and irreversible modification of the mechanical properties of a quenched, initially randomly oriented, material. This is the signature of a transition from a fully randomly oriented sample to an aligned sample.

These results indicate that there is no difference in the rheological response between pure cholesteric samples and those with inclusions, provided the samples remain in a fully randomly oriented state. Any effect of the inclusions on the viscoelastic response of a cholesteric liquid crystal is completely hidden by the response due to the randomly oriented texture. Thus, investigation of the effect of the inclusions on the rheological properties of a cholesteric liquid crystal requires an oriented structure of the liquid crystal phase. This can be achieved by preshearing the sample.

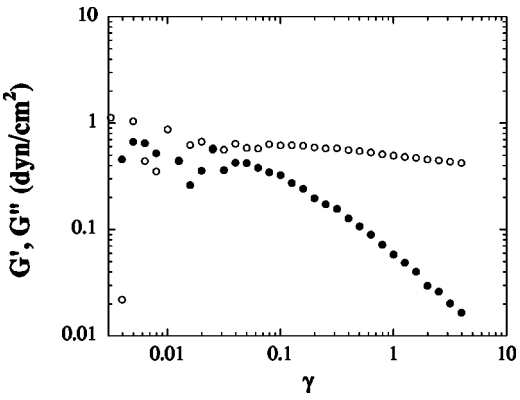

FIG. 6. The strain amplitude dependence of the storage G' (solid circles) and the loss G'' (open circles) moduli for a presheared sample with inclusions. Measurements were performed at a frequency $\omega=1$ rad/sec.

C. Shear-aligned samples

In this second set of experiments, measurements are carried out after strongly preshearing the samples for 500 sec at a shear rate of 10 sec^{-1} and at a temperature of 20 °C. The results of the preceding section imply that a preshear at this rate and duration leads to an alignment of the cholesteric layers in the entire sample. Because of this alignment, all the results reported in this section do not depend on whether or not the sample was quenched before the preshear. We again investigate pure cholesteric samples and cholesteric samples with inclusions. Strain sweep experiments (Fig. 6) confirm that, at $\gamma=0.05$, the measurements of the frequency dependence of the complex modulus described in the preceding section correspond to the linear regime, since up to $\gamma\cong 0.05$, both $G'(\omega)$ and $G''(\omega)$ do not depend on the strain amplitude within experimental precision.

After the preshear, oscillatory measurements show that the viscoelasticity of the pure cholesteric sample is dominated by the viscous part, since over the whole range of frequencies explored, the loss modulus $G''(\omega)$ is larger than the storage modulus $G'(\omega)$ [Fig. 7(a)]: this sample exhibits a fluidlike behavior. For frequencies larger than 10 rad/sec, one observes a behavior typical of a Maxwell fluid: $G''(\omega)=\eta\omega$, with an effective viscosity of $\eta=43$ cP, and $G'(\omega)=\eta\tau\omega^2$, with a relaxation time $\tau=5.6$ msec. The value of η agrees well with the viscosity measured in the shear-rate sweep experiments described in the preceding section. It is, moreover, of the same order of magnitude as the viscosity in a nematic phase [2]. The characteristic relaxation frequency $1/\tau\simeq 200$ rad/sec is higher than the upper limit of the measured frequency range, consistent with our observation of terminal Maxwell-fluid behavior.

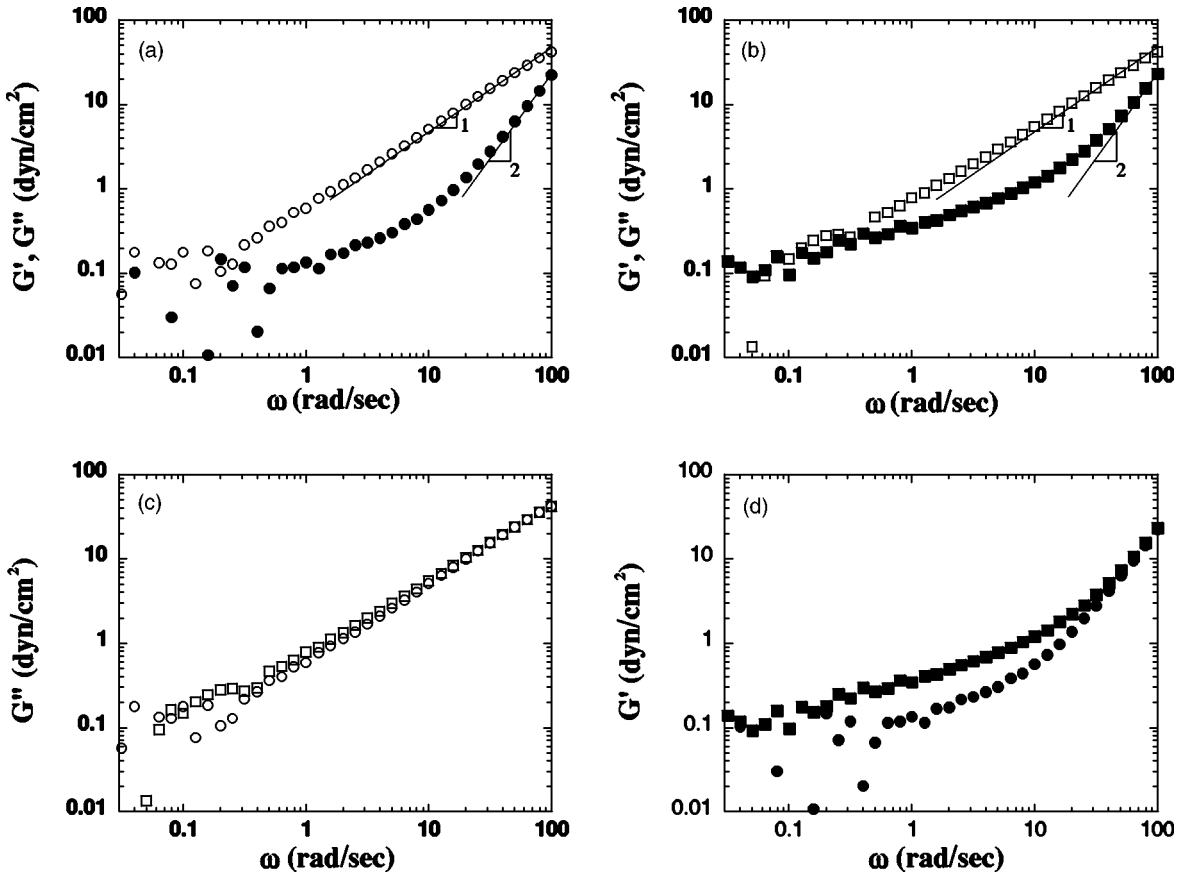

FIG. 7. The frequency dependence of the storage $G'(\omega)$ (solid symbols) and the loss $G''(\omega)$ (open symbols) moduli, for a pure cholesteric sample (circles) and a cholesteric sample with inclusions (squares). The strain amplitude is $\gamma=0.05$. The samples were presheared for 500 sec at a shear rate of $\dot{\gamma}=10\ \mathrm{sec}^{-1}$. (a) $G'(\omega)$ and $G''(\omega)$ for a pure cholesteric sample, (b) $G'(\omega)$ and $G''(\omega)$ for a sample with inclusions, (c) $G''(\omega)$, and (d) $G'(\omega)$, for samples with and without inclusions.

When the same preshear treatment is applied to the cholesteric samples with inclusions, a clear difference is observed (Fig. 7): while the loss modulus remains the same [Fig. 7(c)], the storage modulus of the sample with inclusions increases significantly at low frequencies [Fig. 7(d)]. Moreover, below $\omega=1$ rad/sec, the storage modulus reaches a plateau, $G_0=0.3\ \mathrm{dyn/cm}^2$. In addition, $G'(\omega)$ and $G''(\omega)$ cross at $\omega_c\simeq 0.5$ rad/sec, below which the behavior is elastic, with the storage modulus larger than the loss modulus. These features provide a clear signature of the gel-like behavior of the cholesteric liquid crystal with inclusions, consistent with the predictions that will be given in the theoretical section. Furthermore, the control of the concentration of particles incorporated in the liquid crystal enables us to tune the height of the plateau of the storage modulus and therefore the strength of the gel, as shown in Fig. 8, where two concentrations of particles, with volume fraction of 0.3% and 0.4%, respectively, are used. The loss modulus exhibits only a very weak variation with the particle concentration over the entire range of frequency, while the storage modulus shows a marked increase with particle concentration for frequencies smaller than 20 rad/sec. In particular, the low-frequency plateau modulus increases from 0.2 to 0.4 $\mathrm{dyn/cm}^2$ as the concentration increases.

Pure cholesteric samples and those with inclusions also exhibit markedly different behavior in the shear rate sweep experiments. The effective viscosity of a presheared pure cholesteric sample depends only weakly on the shear rate, as can be seen in Fig. 5. There is a shear thinning of about

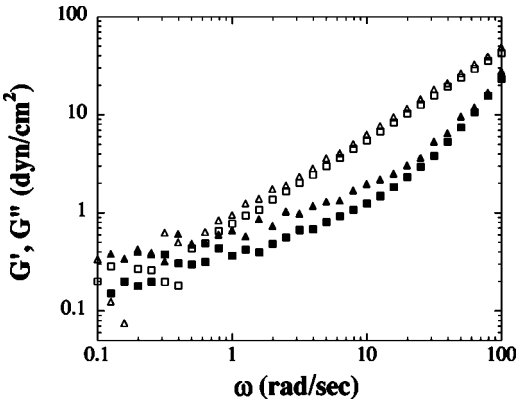

FIG. 8. The frequency dependence of the storage $G'(\omega)$ (solid symbols) and the loss $G''(\omega)$ (open symbols) moduli of cholesteric samples containing inclusions at a volume fraction of 0.3% (squares) and 0.4% (triangles). The strain amplitude is $\gamma=0.05$. Both samples were presheared for 500 sec at $\dot{\gamma}=10\ \mathrm{sec}^{-1}$.

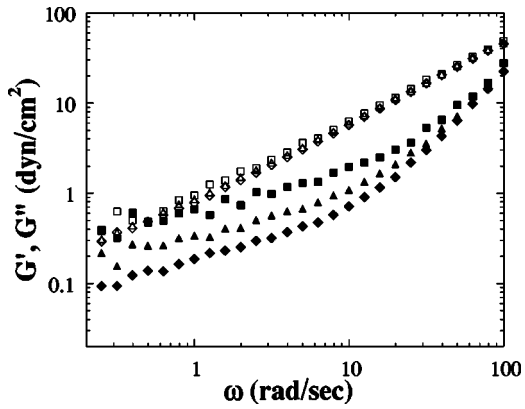

FIG. 9. The frequency dependence of the storage G' (solid symbols) and the loss G'' (open symbols) moduli of cholesteric samples containing inclusions. Measurements were performed with a strain amplitude $\gamma=0.05$ (squares), 0.20 (triangles), and 0.40 (diamonds). The samples were presheared for 500 sec at $\dot{\gamma}=10\ \mathrm{sec}^{-1}$.

20%, and the viscosity reaches the plateau value of 50 cP for rates larger than 5 sec^{-1}. This value is in good agreement with the value derived from the oscillatory experiments (43 cP). Increasing and decreasing rate sweeps result in exactly the same behavior. These data can also be superimposed on those obtained from a quenched sample when the shear rate is decreased.

Presheared samples with inclusions give results in clear contrast with those of pure cholesteric samples. The samples containing colloidal particles display a shear-thinning behavior: the apparent viscosity decreases from 180 cP down to 57 cP, this value being reached at about 10 sec^{-1}. The shear-thinning behavior appears much more pronounced than in the case of a pure cholesteric presheared sample (more than 200% compared to 20%). It is, nevertheless, much less pronounced than it is in a quenched pure cholesteric sample; however, by contrast, it is permanent, with two consecutive measurements giving the same results.

To investigate the nonlinear viscoelastic regime of presheared samples with inclusions, oscillatory measurements are made at a frequency $\omega=1$ rad/sec and for increasing strain amplitudes, γ, from 0.05 to 0.4. We note (Fig. 6) that the decrease of $G'(\omega)$ with increasing γ starts at a lower strain amplitude and is more pronounced than the decrease of $G''(\omega)$. In the nonlinear regime, the frequency dependence of $G'(\omega)$ and $G''(\omega)$ for each value of γ is shown in Fig. 9. In the range of γ investigated, the loss modulus $G''(\omega)$ decreases weakly when γ increases, while the storage modulus $G'(\omega)$ varies much more strongly. This is consistent with what is observed in the strain-sweep measurements. We note that if a measurement at low strain amplitude ($\gamma=0.05$) is repeated after one at large amplitude, the results obtained from the two measurements at low amplitude are identical.

When aligned by preshear, pure cholesteric samples and samples containing inclusions exhibit markedly different rheological behavior. In particular, linear oscillatory measurements show a transition from a fluidlike behavior to a gel-like behavior arising from the presence of inclusions [1]. As will be discussed in the theoretical section, this gel-like behavior is consistent with the picture of a connected network of linear defects under tension, the network being stabilized by the inclusions located at the nodes. Moreover, both the steady-rate experiments and the oscillatory experiments performed in the nonlinear regime show that large strain amplitudes or strong shear rates do not lead to irreversible changes of the viscoelastic response. This suggests that they do not induce permanent modifications of the defect network, such as breaks of the linear defects or irreversible disconnections of the defects from the nodes.

IV. DISCUSSION

A. Theoretical considerations

The experiments described in the preceding section suggest that presheared bulk cholesteric samples with colloidal inclusions contain a stabilized three-dimensional network of defects of the oily-streak type. The structure of the oily-streak network is reminiscent of that of crosslinked macromolecular solids: the defects play the role of polymers, while the colloidal inclusions located at the nodes of the oily-streak network play the role of chemical crosslinks. On appropriate time scales [11], the defect structure can be viewed as a crosslinked network of elastic bonds that exert forces (determined by the defect line tension $\mathcal{T}$) at the network nodes. We can therefore expect similarities between the mechanical properties of the oily-streak network and those of rubber materials [12].

It is also immediately clear, however, that there are important limitations on the analogy between macromolecular gels and oily-streak networks. First, at low deformation amplitude and frequency, the force-extension law for the links in the case of rubber is Hookean (i.e., their line tension increases in proportion to their extension), while the line tension of the oily streaks is *independent* of their length. Second, the origin of elasticity of the macromolecular links in rubber is purely entropic. In contrast, the line tension of an oily streak is of the order of K, where K is the cholesteric elastic constant. The characteristic energy scale for deformation of an oily-streak link, Kp (where p is the cholesteric pitch), exceeds thermal energies by several orders of magnitude.

It is useful to contrast the behavior of macromolecular and of oily-streak networks in a *step-stress* experiment. When a step stress is applied to rubber in equilibrium, it deforms until the applied stress is balanced by the induced stress arising from the anisotropy of the distribution of links and the increased line tension of the extended links. The ratio of the applied stress to the resultant strain determines the shear modulus G. A different behavior is expected to occur in the case of the oily-streak network, as the maximum stress generated by one link is now extension independent. A high-enough applied stress (exceeding the yield stress σ_y) thus cannot be counteracted by induced stresses, and the material will flow: the node locations will continue displacing and the streaks extending until the criterion for a substantial topological rearrangement or rupture of the network is reached. Thus the oily-streak network behaves as a viscoplastic solid, or ''Bingham fluid'' [13].

TABLE I. Values of fit parameters G_0, $\beta_d(\gamma)$, and $\beta_o(\gamma)$ in $G'(\omega,\gamma)=G_0(\gamma)+\beta_d(\gamma)\omega^{1/2}+\beta_o(\gamma)\omega^2$ [Eq. (2)] for presheared and nonpresheared samples measured at different strain amplitudes γ. The fits are shown in Figs. 10 and 12.

Sample	γ	G_0	β_d (dyn/cm^2 sec$^{1/2}$)	$\beta_o(\gamma)$(P sec)
Nonpresheared	0.05	0.75	1.68	2.42×10^{-3}
Presheared with no inclusions	0.05	0.065	0.11	2.14×10^{-3}
Presheared with inclusions	0.05	0.27	0.42	2.25×10^{-3}
	0.20	0.050	0.27	2.10×10^{-3}
	0.30	0.054	0.19	2.12×10^{-3}
	0.40	0.010	0.17	2.08×10^{-3}

The elastic shear modulus at low frequencies and amplitudes, G_0, of an oily-streak network can be estimated using arguments analogous to those used for rubber elasticity [12]. These predict $G_0\simeq nw/3$, where w is the strain energy stored in one network element and $n\simeq d_{\rm net}^{-3}$ is their number density, with $d_{\rm net}$ the average mesh size of the elastic network. For oily-streak defects with line tension $\mathcal{T}$, $w=\mathcal{T}d_{\rm net}$, and $G_0\simeq\mathcal{T}/d_{\rm net}^2$. Taking $\mathcal{T}\simeq10\ K\simeq10^{-5}$dyn and $d_{\rm net}=50\ \mu$m, we obtain $G_0\simeq0.4$ dyn/cm^2. This corresponds to a very weak gel.

Note that in this section, we have considered only stresses directly generated by the network of oily-streak defects. The elastic and viscous moduli of a real cholesteric liquid crystal will be influenced by contributions arising from the intrinsic viscoelasticity of a nondeformed cholesteric liquid crystal and from possible quenched-in textures of non-oily-streak type. We will allow for these contributions in the following section.

B. Data analysis

In the experiments (Sec. III), the pure cholesteric sample exhibits a typical ''terminal'' behavior of a Maxwell fluid for $\omega\geqslant10$ rad/sec: $G''(\omega)=\omega\eta$ with effective viscosity $\eta=43$ cP and $G'(\omega)=\omega^2\eta\tau$ with relaxation time $\tau=5.6$ msec. This value of τ agrees well with the characteristic relaxation time of the director, $\tau_{\rm dir}=(\gamma_1/K)(p/4\pi)^2\simeq6.7$ msec. When colloidal inclusions are added, the Maxwell-fluid behavior characteristic of the pure cholesteric sample persists for $\omega\geqslant50$ rad/sec. At lower frequencies, however, $G'(\omega)$ exhibits a pronounced increase compared to the pure cholesteric case, while $G''(\omega)$ is not changed. This reflects the elasticity of the oily streak defects present in the sample. Below $\omega=1$ rad/sec, we observe a plateau in the storage modulus $G'(\omega)$ of magnitude $G_0=0.3$ dyn/cm^2. The value of G_0 is consistent with the prediction given above. Furthermore, the curves for $G'(\omega)$ and $G''(\omega)$ cross at $\omega\simeq\omega_g=0.5$ rad/sec, and to within experimental precision, $G'(\omega)>G''(\omega)$ for $\omega<\omega_g$. This provides a signature of *gel-like* behavior and is consistent with our model of a particle-stabilized defect network.

We stress that even though ''misaligned'' regions, where cholesteric layers are oriented at a nonzero angle with respect to shear and are therefore compressed, do exist in the vicinity of the colloidal inclusions and in the center of the oily streaks, their deformation relaxes on short time scales, and such regions are not responsible for the observed solidlike behavior in the presheared samples. These regions are, however, expected to give contributions of the form $G'(\omega)\sim\omega^{1/2}$ and $G''(\omega)\sim\omega^{1/2}$ at intermediate frequencies [14]. The nonzero value of the low-frequency storage modulus G_0 arises primarily from the presence of the connected network of linear objects with nonzero line tension, the deformation of which cannot fully relax.

The theoretical discussion given above suggests that the frequency dependence of the storage modulus G' in presheared samples with colloidal inclusions can be described as a sum of three contributions: G_0 arising from the zero-frequency shear modulus of the defect network, $\beta_d\omega^{1/2}$ arising from the disoriented (misaligned) parts of the sample, and $\beta_o\omega^2$ arising from the regions of the sample where the layers are parallel to the shear direction (i.e., most of the sample). Thus we can write

$$G'(\omega)=G_0+\beta_d\omega^{1/2}+\beta_o\omega^2, \tag{2}$$

with $G_0\simeq\mathcal{T}/d_{\rm net}^2$ and $\beta_o\simeq\eta(\gamma_1/K)(p/4\pi)^2$. As for β_d, we estimate its value using the result $G'\simeq(\pi/24\sqrt{2})\sqrt{(B\eta)}\,\omega^{1/2}$ derived for fully disoriented lamellar phases [14]. For a cholesteric liquid crystal, $B=K(2\pi/p)^2$. Moreover, in our samples, only part of the sample, is expected to be in the disoriented state. We define ζ as the fraction of the sample in a disoriented state. To a first order of approximation, we can assume β_d to be proportional to ζ; we therefore expect $\beta_d\simeq\zeta(\pi^2/12\sqrt{2}p)\sqrt{(K\eta)}$.

A similar analysis can be performed for the loss modulus $G''(\omega)$. In this case, we do not expect a plateau contribution at low frequencies, we, however, expect the ordered part of the sample to result in a Maxwell-fluid type contribution linear in ω, and the disoriented parts of the sample to result in a $\omega^{1/2}$ contribution, of the same magnitude as in the case of $G'(\omega)$ [14]. We therefore write

$$G''(\omega)=\alpha_d\omega^{1/2}+\alpha_o\omega, \tag{3}$$

where the theoretically expected values are $\alpha_o=\eta$ and $\alpha_d=\beta_d=\zeta(\pi^2/12\sqrt{2}p)\sqrt{(K\eta)}$ [14]. These functional forms can be fit to our data to describe the full frequency dependence of $G'(\omega)$ and $G''(\omega)$.

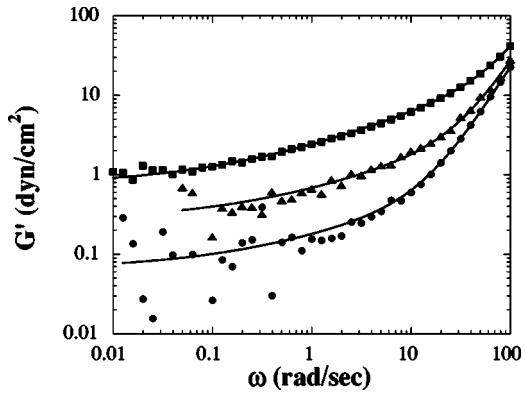

FIG. 10. The frequency dependence of the storage modulus G' for a pure cholesteric sample submitted to a temperature quench (squares), for a presheared cholesteric sample without inclusions (circles) and a presheared sample with inclusions (triangles). The strain amplitude is $\gamma=0.05$. The solids lines are the fits of the data to Eq. (2). The values of the parameters obtained from the fit are listed in Table I.

1. Linear regime

The results of fitting our data for the storage modulus G' in the linear viscoelastic regime ($\gamma=0.05$) to Eq. (2) are displayed in Table I. For the presheared sample with inclusions, a good fit of the data is obtained across the entire measured frequency range, as shown in Fig. 10. We obtain $G_0=0.266$ dyn/cm^2, $\beta_d=0.416$ dyn/cm^2 sec$^{1/2}$, $\beta_o=2.25\times10^{-3}$ dyn/cm^2 sec^2. The values of G_0 and β_o are consistent with theoretical expectations. As for the parameter β_d, the theoretical expectation with $p=15$ μm, $K=10^{-6}$ dyn, $\eta=43$ cP is $\beta_d\simeq\zeta\times1.5$ dyn/cm^2 sec$^{1/2}$, corresponding to ζ of the order of 0.1.

We now repeat the fitting procedure for G' measured in the nonpresheared sample and in the presheared sample with inclusions. In both cases, the quality of the fit is comparable to the case of the presheared sample with inclusions (Fig. 10). For the presheared sample without inclusions,

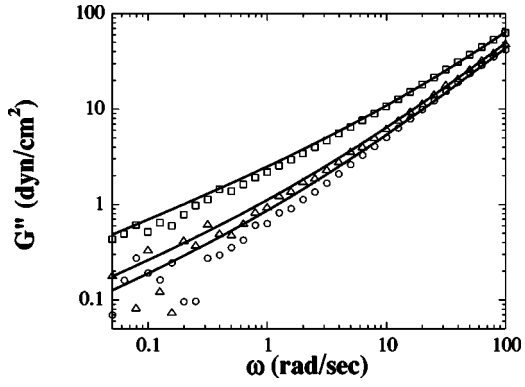

FIG. 11. The frequency dependence of the loss modulus G'' for a pure cholesteric sample submitted to a temperature quench (squares), for a presheared cholesteric sample without inclusions (circles) and a presheared sample with inclusions (triangles). The strain amplitude is $\gamma=0.05$. The solids lines are the fits of the data to Eq. (3). The values of the parameters obtained from the fits are listed in Table II.

TABLE II. Values of fit parameters $\alpha_d(\gamma)$ and $\alpha_o(\gamma)$ in $G''(\omega,\gamma)=\alpha_d(\gamma)\omega^{1/2}+\alpha_o(\gamma)\omega$ [Eq. (3)] for presheared and nonpresheared samples measured at different strain amplitudes γ. The fits are shown in Fig. 11.

Sample	γ	α_d(dyn/cm^2 sec$^{1/2}$)	$\alpha_o(\gamma)$(P)
Nonpresheared	0.05	2.1	0.44
Presheared with no inclusions	0.05	0.48	0.39
Presheared with inclusions	0.05	0.70	0.42
	0.20	0.65	0.41
	0.30	0.61	0.41
	0.40	0.57	0.41

the fit parameters are $G_0=0.065$ dyn/cm^2, $\beta_d=0.11$ dyn/cm^2 sec$^{1/2}$, $\beta_o=2.14\times10^{-3}$ dyn/cm^2 sec^2. Note that the value of G_0 is significantly lower than in the sample with inclusions, indicating that the average distance between defects increases in the absence of inclusions; this agrees with our expectation that inclusions make the density of defects increase by stabilizing these defects. For the nonpresheared sample, the fit parameter values are $G_0=0.75$ dyn/cm^2, $\beta_d=1.68$ dyn/cm^2 sec$^{1/2}$, $\beta_o=2.42\times10^{-3}$ dyn/cm^2 sec^2. The value of G_0 is larger than in nonpresheared samples but remains one order of magnitude below the bulk compression modulus $B\simeq10$ dyn/cm^2 [15]. The values of β_o are identical in the three cases, as expected for an intrinsic property of a cholesteric liquid crystal. The value of β_d in the nonpresheared sample is significantly larger than in both presheared samples. Since we expect β_d to be proportional to the relative volume ζ of the sample that is in the disoriented state, the values listed in Table I imply that ζ for the presheared sample with no inclusions is 15 times smaller than for the nonpresheared sample. For the presheared sample with inclusions, ζ is four times larger than without inclusions; this can be attributed to the presence of disordered regions associated with the defect network.

The data for the frequency dependence of the loss modulus $G''(\omega)$ for the same three samples discussed above are fitted using Eq. (3). The results of the fits are displayed in Fig. 11 and in Table II. The fit of the data for $G''(\omega)$ with Eq. (3) is generally of lower quality as compared to the fit for $G'(\omega)$ with Eq. (2). The value of the effective viscosity α_o, however, varies only slightly (from 39 cP to 44 cP) and is consistent with all other cases. Theoretically, one expects [14] the contributions from the disoriented regions to $G'(\omega)$ and $G''(\omega)$ to be identical: $\alpha_d=\beta_d$ in each sample. Although not strictly equal, the values of α_d extracted from our fits are indeed comparable to the values of β_d. Furthermore, α_d values show the same trends as those for β_d: α_d for the nonpresheared sample is significantly higher than for the presheared sample with inclusions, which in turn is higher than α_d for the presheared sample without inclusions.

We conclude that Eq. (2) and Eq. (3) adequately describe our data for, respectively, the storage modulus $G'(\omega)$ and the loss modulus $G''(\omega)$ in the linear viscoelastic regime, and, furthermore, that the values of the fit parameters are overall consistent with theoretical expectations.

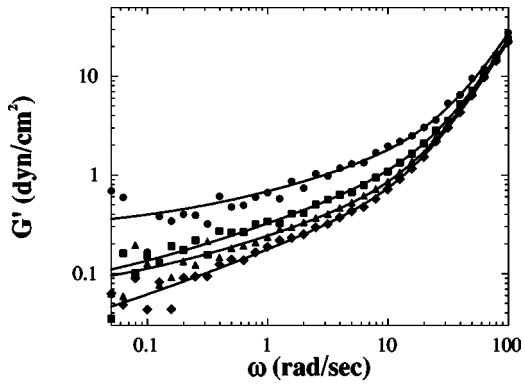

FIG. 12. The frequency dependence of the storage modulus G' for a cholesteric sample with inclusions submitted beforehand to a preshear (for 500 sec at a shear rate of $\dot{\gamma}=10\ \mathrm{sec}^{-1}$). Measurements were performed with maximum strain amplitudes of $\gamma=0.05$ (circles), 0.20 (squares), 0.30 (triangles), and 0.40 (diamonds). The solids lines are the fits of the data with Eq. (2). The values of the parameters obtained from the fits are listed in Table I.

2. Nonlinear regime

Equations (2) and (3) are also used to analyze the data in the nonlinear regime, attained at higher maximum shear strain amplitudes, for the presheared sample with inclusions. The fits of $G'(\omega)$ are shown in Fig. 12 and the results of the fits of both $G'(\omega)$ and $G''(\omega)$ are summarized in Tables I and II. The parameters β_o and α_o, which characterize the intrinsic viscoelasticity of the cholesteric liquid crystal, remain constant in the entire range of strain amplitude investigated ($\gamma=0.05$ to $\gamma=0.4$). This shows that, in this range of γ, the intrinsic response of a cholesteric liquid crystal remains in the linear regime, and therefore the nonlinear contributions arise mainly from the network of defects. The loss modulus $G''(\omega)$ exhibits a much weaker variation with γ than the storage modulus $G'(\omega)$ (Fig. 9). Thus, we focus on the behavior of $G'(\omega,\gamma)$.

We find that the zero-frequency shear modulus G_0 is significantly smaller for $\gamma\geqslant 0.2$ than for $\gamma=0.05$. This may be a consequence of the $1/\gamma$ dependence of the crossover frequency ω_c predicted theoretically.

In addition, strain sweep experiments were carried out with strain amplitudes γ up to 4, for different fixed frequencies ($\omega=0.1$ rad/sec, $\omega=0.3$ rad/sec, and $\omega=1$ rad/sec). The results are summarized in Fig. 13, where we show that the product $\gamma G'(\omega,\gamma)$ is essentially γ independent for maximum strain amplitudes larger than 0.2. We find that $\gamma G'(\omega,\gamma)\simeq\sigma_y(\omega)$. Furthermore, $\sigma_y(\omega)$ is found to vary linearly with the frequency (see inset of Fig. 13). The zero-frequency limit of $\sigma_y(\omega)$ defines the yield stress σ_y, for which we obtain a value of $0.015\ \mathrm{dyn/cm}^2$. By contrast, from the values in Table I, it can be seen that, in the range $\gamma\geqslant 0.2$, and $1\leqslant\omega\leqslant 10$ rad/sec, $G'(\omega,\gamma)$ is dominated by the contribution $\beta_d\omega^{1/2}$ arising from the disoriented parts of the sample. The β_d dependence itself can be fitted to the form $G_f/(1+\gamma/\gamma_c)$ (Fig. 14) introduced by Colby [10]. Here, the parameter $G_f(\omega)$ has the meaning of $G'(\omega)$ in the linear viscoelastic regime ($\gamma\leqslant 0.05$ in our case) and γ_c has the meaning of a *yield strain*. We obtain $G_f=0.53\ \mathrm{dyn/cm}^2$ and $\gamma_c=0.18$. There follows a prediction for the value of the yield stress in our material: $\sigma_y=\gamma_c G_f\simeq 0.05\ \mathrm{dyn/cm}^2$, in reasonable agreement with the value of σ_y directly determined from the strain sweep experiments. This provides a nontrivial crosscheck of the consistency of our interpretation of the data.

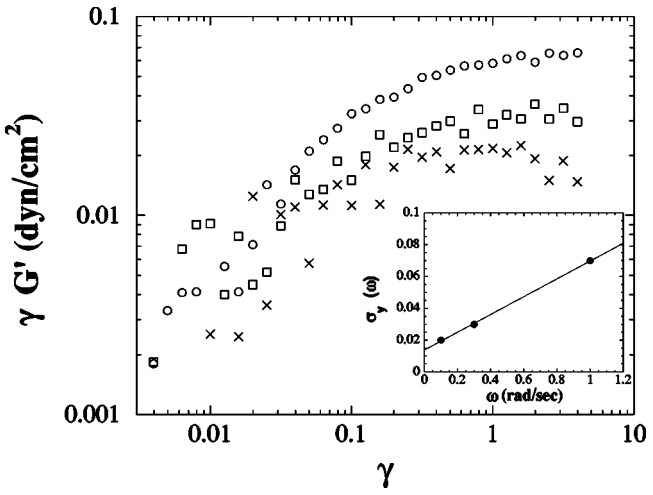

FIG. 13. The maximum-strain-amplitude dependence of the storage modulus G' times the strain γ for a presheared sample with inclusions. Measurements were performed at frequencies of $\omega=0.1$ rad/sec (crosses), $\omega=0.3$ rad/sec (squares), $\omega=1$ rad/sec (circles). Inset, plateau in $G'\gamma$ as a function of the frequency ω. The solid line is a linear fit of the data.

V. CONCLUSIONS

We have studied the rheological properties of cholesteric liquid crystals and related the viscoelastic behavior to the defect structures of the samples. This defect structure can be controlled by the introduction of colloidal particles into a cholesteric liquid crystal. A simple model accounting for both the intrinsic viscoelasticity of the cholesteric liquid crystal and the viscoelasticity arising from the defect struc-

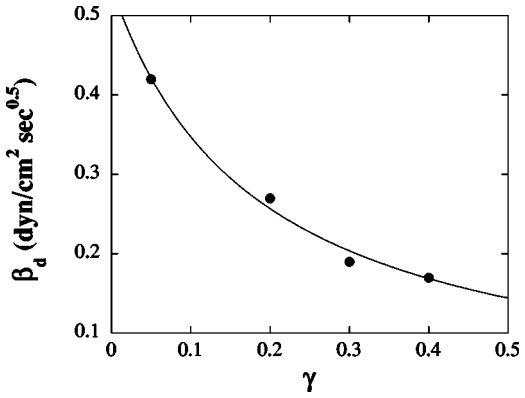

FIG. 14. The fit parameter, β_d, as a function of the strain amplitude γ. The values of β_d are derived from the fits of $G'(\omega,\gamma)$ for presheared samples with inclusions (Fig. 12). The solid curve shows a fit of $\beta_d(\gamma)$ by the function $G_f/(1+\gamma/\gamma_c)$ [10], with $G_f=0.53\ \mathrm{dyn/cm}^2$ and $\gamma_c=0.18$.

ture allows us to fit the frequency dependence of the complex moduli in both the linear and the nonlinear regimes. The fit parameters are discussed in terms of the defect structure which exists in presheared and nonpresheared samples, with or without inclusions. A presheared sample without inclusions exhibits a fluidlike behavior, while a presheared sample with inclusions displays a gel-like behavior, with an increase of the elastic modulus G' at low frequency. We interpret this increase of G' as a signature of a network of linear defect under tension. This defect-mediated increase of the elastic modulus of layered media is intrinsically different from that obtained when particles are dispersed in systems such as polymer solutions and melts [17,18], which have no long-range order and do not support defect structures. It is also different from the solidlike rigidity observed in macroscopically disordered samples of layered phases [9,10], whose origin is bulk region with layers unfavorably aligned relative to the shear direction. In these cases, the rigidity cannot survive shear-induced alignment of the randomly oriented regions; in contrast, the defect network stabilized by colloidal inclusions and its solidlike elasticity are not destroyed by such shear alignment.

ACKNOWLEDGMENTS

We thank Philippe Poulin for key participation in our studies of the structure and the stability of oily-streak defect networks [1], as well as his role in the initiation of our rheological studies. We also thank Veronique Trappe for advice on and help with the rheology. This work was supported primarily through NSF Grant No. DMR95-07366, as well as the Bourse Lavoisier du Ministère Français des Affaires Etrangères.

[1] M. Zapotocky, L. Ramos, P. Poulin, T.C. Lubensky, and D.A. Weitz, Science **283**, 209 (1999).
[2] P.-G. de Gennes and J. Prost, *The Physics of Liquid Crystals* (Clarendon, Oxford, 1993).
[3] To avoid confusion, we stress that unlike the case of smectic layers, the notion of *cholesteric* layer has no connection to the translational order of the molecules. The positions of the cholesteric layers are determined purely by the orientational order of the molecules. It is also worth noting that while the orientation of the molecules in the smectic-*A* phase is by definition always perpendicular to the smectic layers, in the cholesteric phase the orientation of the molecules is always *parallel* to the cholesteric layers.
[4] See, e.g., M. Kléman, *Points, Lines, and Walls* (Wiley, Chichester, 1983).
[5] T.C. Lubensky, Phys. Rev. A **6**, 452 (1972).
[6] M. Zapotocky, L. Ramos, P. Poulin, T.C. Lubensky, and D.A. Weitz (unpublished).
[7] H.E. Warriner *et al.*, Science **271**, 969 (1996); J. Chem. Phys. **107**, 3707 (1997); S.L. Keller *et al.*, Phys. Rev. Lett. **78**, 4781 (1997).
[8] G. Basappa, Suneel V. Kumaran, P.R. Nott, S. Ramaswamy, V.M. Naik, and D. Rout, Eur. Phys. J. B **12**, 269 (1999).
[9] R.G. Larson *et al.*, Rheol. Acta **32**, 245 (1993).
[10] R.H. Colby *et al.*, Rheol. Acta **36**, 498 (1997).
[11] That is, time scales longer than the characteristic director relaxation time $\tau_{\mathrm{dir}} \simeq (\gamma_1/K)(p/4\pi)^2$ at the cholesteric Brillouin zone edge and shorter than the typical lifetime of the nodes of the defect network.
[12] L.R.G. Treloar, *The Physics of Rubber Elasticity* (Clarendon, Oxford, 1975).
[13] J.P. Friend and R.J. Hunter, J. Colloid Interface Sci. **37**, 548 (1972).
[14] K. Kawasaki and A. Onuki, Phys. Rev. A **42**, 3664 (1990).
[15] The fact that the value of G_0 in a nonpresheared sample remains one order of magnitude below the bulk compression modulus may very well indicate that the compressed disoriented regions are relaxing largely through bending, departing from the framework of Ref. [14]. This framework depends on the assumption that the scales on which layers are deformed are significantly larger than the layer spacing, which will not be true if they are quench-in sharp boundaries between various orientations from sample preparation, like in the case of a close packing of multilamellar vesicles [16].
[16] P. Panizza *et al.*, Langmuir **12**, 248 (1996).
[17] L.E. Nielsen and R.F. Landel, *Mechanical Properties of Polymers and Composites*, 2nd ed. (Dekker, New York, 1994), Chap. 7.
[18] M.R. Kamal and A. Mutel, J. Polym. Eng. **5**, 293 (1985).